NJC

Accepted Manuscript

This is an *Accepted Manuscript*, which has been through the Royal Society of Chemistry peer review process and has been accepted for publication.

Accepted Manuscripts are published online shortly after acceptance, before technical editing, formatting and proof reading. Using this free service, authors can make their results available to the community, in citable form, before we publish the edited article. We will replace this *Accepted Manuscript* with the edited and formatted *Advance Article* as soon as it is available.

You can find more information about *Accepted Manuscripts* in the Information for Authors.

Please note that technical editing may introduce minor changes to the text and/or graphics, which may alter content. The journal's standard Terms & Conditions and the Ethical guidelines still apply. In no event shall the Royal Society of Chemistry be held responsible for any errors or omissions in this *Accepted Manuscript* or any consequences arising from the use of any information it contains.

ROYAL SOCIETY OF CHEMISTRY

www.rsc.org/njc

Synthesis of Pd(II) organometal incorporated ordered Im3m mesostructural silica and catalytic activity in water-medium Sonogashira reaction

Fengxia Zhu, Lili Zhu, Xiaojun Sun, Litao An*, Pusu Zhao*, Hexing Li

Received (in XXX, XXX) Xth XXXXXXXXX 200X, Accepted Xth XXXXXXXXX 200X
First published on the web Xth XXXXXXXXX 200X
DOI: 10.1039/b000000x

A novel and reusable Pd(II) organometal functionalized SBA-16 catalyst was synthesized by co-condensation of $Pd[PPh_2(CH_2)_2Si(OCH_2CH_3)_3]_3Cl_2$ and tetraethyl orthosilicate (TEOS). This catalyst displayed bicontinuous cubic Im3m mesostructure channel, which ensured the convenient diffusion of reactant molecules into the pore channels. The catalyst exhibited very high activity for Sonogashira coupling reaction of aryl halides with phenylacetylene in water medium. Moreover, the synthesized catalyst could be separated from the reaction mixture by simple filtration and reused up to five runs without significant loss in activity.

1. Introduction

The Sonogashira coupling reaction of acetylene with aryl halides catalyzed by Pd(II) complexes is a powerful tool in organic synthesis and has been widely applied to various areas such as biologically active molecules, natural product synthesis and materials science.[1-4] This reaction is usually performed in homogenous system with organic solvent, palladium-phosphorous complex.[5-7] Using of toxic organic solvents such as DMSO, DMF and acetonitrile, etc. in Sonogashira coupling reaction not only increases the cost of experiment, but also pollutes the environment. Water is cheap, nontoxic, and not flammable which could be considered as an alternative to expensive organic solvents and an attractive media for the development of environmentally harmless chemical processes. Furthermore, separation of water-insoluble organic compounds from the aqueous phase is very easy in many cases [8].

Recently, homogenous Pd complex catalysts are also employed in water-medium organic reactions, which could diminish environmental pollution from organic solvents.[9,10] Though the high activity and selectivity, the homogeneous palladium organometallic catalysts usually show disadvantages in separation and recycling. Moreover, the reaction suffers from severe problems related to the separation, recovery, and recycling of the expensive, toxic metal catalysts, etc.[11]

In this regard, different types of heterogeneous catalysts have been prepared with the goal to achieve catalyst recovery and recycling for water-medium Sonogashira coupling reaction, such as PVC-supported Pd nanoparticles,[12] polystyrene resin-supported Pd(II) complex catalyst,[13] polymer supported macrocyclic Schiff base palladium complex,[14] organopalladium(II) immoblized silicas,[15] and so on.

It is obvious that the functionalized supports are used to immobilize palladium complex catalysts, which show higher activities than homogeneous catalysts in the Sonogashira coupling reaction in water.[16-19] Among different supports used for immobilized Pd(II) homogeneous catalyst, mesoporous silica materials remain the most popular choice because of their relatively low cost, large surface area, high thermal, mechanical stability and good catalytic performance.[20] SBA-15 and MCM-41 are the representative example for these types of materials and have been used as supports for palladium catalysts.[17,21-23]

Compared with two-dimensional hexagonal mesoporous materials such as SBA-15, the mesoporous material SBA-16 (cubic, Im3m)[24] provides a new possible candidate for the solid support for the immobilization of heterogeneous catalysts. Because of the large surface area, interesting 3D structure consisting of ordered and interconnected spherical mesopores make it easy accessible for guest molecules, which facilitates the transport of reactants and products without pore blockage.[25-28] Up to now, most SBA-16 supported Pd heterogeneous catalysts were prepared by either post-grafting or impregnation method, while the organic functionalities terminally bonded to the pore surface might partially block the pore channels, which might disfavor the catalytic efficiency.[28, 29] Moreover, they would easily suffer from leaching during liquid phase reactions, leading to the poor durability.[29]

In this paper, we report the synthesis of a functionalized SBA-16 with Pd(II) organometals incorporating into silica framework by surfactant-directed co-condensation between the tetraethoxysilane (TEOS) and Pd(II)organometallicsilane. This functionalized mesoporous material not only acts as an effective palladium

[a] *Address: Jiangsu Key Laboratory for Chemistry of Low-Dimensional Materials, Huaiyin Normal University, Huaian, 223300 P. R. China. Fax: + 86 517 83525083; Tel: + 86 517 83525377; E-mail: anlitao@hotamil.com; zhaopusu66@sohu.com*

catalyst for the water-medium Sonogashira coupling reaction, but also can be reused for five times without obvious loss of catalytic activity. Its activity is higher than the analogous catalysts which are prepared from SBA-15.

2. Experimental

2.1. Catalyst preparation

Firstly, the $Pd[PPh_2(CH_2)_2Si(OCH_2CH_3)_3]_2Cl_2$ was synthesized by mixing 10 mL of toluene, 3.5 mmol of $Pd(COD)Cl_2$ and 0.70 mmol of $PPh_2CH_2CH_2Si(OCH_2CH_3)_3$ under argon atmosphere, followed by stirring at 30 °C for 3 h. After being concentrated to 6.0 mL pentane is added, leading to $Pd[PPh_2(CH_2)_2Si(OCH_2CH_3)_3]_2Cl_2$. Then, the organopalladium(II) functionalized SBA-16, denoted as Pd(II)-PMO-SBA-16, was prepared by co-condensation method. In a typical synthesis, 1.0 g of F127 and 2.6 g K_2SO_4 was dissolved in 30 g of 0.50 M HCl solution with stirring at 38 ^oC. After complete dissolution, 4.5 g of tetraethyl orthosilicate (TEOS) was added to the homogeneous solution. After being prehydrolyzed for 1 h, 0.42 g of $Pd[PPh_2(CH_2)_2Si(OCH_2CH_3)_3]_2Cl_2$ was added into the solution. This mixture was left under vigorous stirring at 38 ^oC for 24 h. Subsequently, hydrothermal treatment of the reactant mixture was carried out at 100 ^oC for 24 h under static conditions in a closed polypropylene bottle. Finally, the surfactants and other organic substances were extracted by refluxing in ethanol solution at 80 ^oC for 24 h. The Pd(II) loading was determined as 3.2 wt% by ICP analysis.

For comparison, the organopalladium(II) functionalized SBA-15, denoted as Pd(II)-PMO-SBA-15 was also prepared by surfactant-directed co-condensation of $Pd[PPh_2(CH_2)_2Si(OCH_2CH_3)_3]_2Cl_2$ and TEOS. Briefly, 0.5 g of P123 was dissolved in 15 g of 2.0 M HCl solution and 3.9 g of distilled water, 1.0 g of TEOS was added at 40 °C. After being prehydrolyzed for 1 h, 0.14 g of $Pd[PPh_2(CH_2)_2Si(OCH_2CH_3)_3]_2Cl_2$ was added into the solution. The mixture was left under stirring for 24 h at 40 ^oC, and subsequently heated for another 24 h at 100 ^oC under static conditions in a closed polypropylene bottle. The yellow solid product was collected and extracted in ethanol solution at 80 ^oC. The Pd(II) loading was determined as 2.9 wt% by ICP analysis.

2.2. Characterization

The compositions and Pd(II) loadings were determined by elemental analysis (Elementar Vario ELIII, Germany) and inductively coupled plasma optical emission spectrometer (ICP-OES, Varian VISTA-MPX). Fourier transform infrared (FTIR) spectra were collected on a Nicolet Magna 550 spectrometer by using the KBr method. Solid-state NMR spectra were recorded on a Bruker AV-400 spectrometer. Thermogravimetric analysis and differential thermal analysis (TG/DTA) were conducted on a DT-60. Low-angle X-ray powder diffraction (XRD) patterns were obtained on a Rigaku D/maxr B diffractometer with Cu Ka. N_2 adsorption–desorption isotherms were measured at 77 K on a Quantachrome NOVA 4000e analyzer, from which the specific surface area (S_{BET}) was calculated by applying Brunauer-Emmett-Teller (BET) method and Barrett-Joyner-Halenda (BJH) model on the adsorption branches, respectively. Meanwhile, the average pore diameter (D_P) and total pore volume (V_P) were calculated from the adsorption isotherms using Barrett-Joyner-Halenda (BJH) model. Surface morphologies and porous structures were observed through a transmission electron microscopy (TEM, JEOL JEM2011). The surface electronic states were analyzed by X-ray photoelectron spectroscopy (XPS, Perkin-Elmer PHI 5000C). All the binding energy (BE) values were calibrated by using the standard BE value of contaminant carbon (C_{1S} = 284.6 eV) as a reference.

2.3. Activity test

A mixture of 1.0 mmol aryl halide, 1.5 mmol phenylacetylene, 0.40 mL 1,8-diazabicyclo[5.4.0] undec-7-ene (DBU), 0.16 mmol CuI, 2.0 mmol n-decane as an internal standard, 4.0 mL H_2O and catalyst with 0.0060 mmol Pd(II) in the flask were stirred at 90 ^oC for a given time. After the reaction was completed, the products were extracted by acetic ether, followed by analysis on a gas chromatograph (SHIMADZU, GC-17A) equipped with a JWDB-5, 95% dimethyl 1-(5%)-diphenylpolysiloxane column and a FID detector. The column temperature was programmed from 80 to 250 ^oC at a ramp speed of 10 ^oC/min. N_2 was used as carrier gas. The reproducibility was checked by repeating each result at least three times and was found to be within ± 5 %.

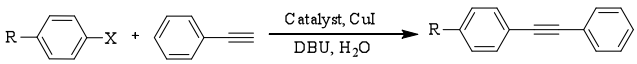

Scheme 1 Chemical equation of Sonogashira between aryl halide and phenylacetylene.

2.4. Catalyst recycling

A mixture of iodobenzene (1.0 mmol), phenylacetylene (1.5 mmol), DBU (0.40 mL), CuI (0.16 mmol), H_2O (4.0 mL) and Pd(II)-PMO-SBA-16 was stirred at 90 ^oC. At the end of reaction, the mixture was cooled to room temperature and filtered to obtain the Pd(II)-PMO-SBA-16 catalyst. The separated catalyst was washed with ethanol and dried under vacuum at 60 ^oC. The catalyst was separated from liquid phase by high-speed centrifugation. After this, the catalyst was reused with fresh charge of reactants for subsequent recycle under the identical reaction conditions.

3. Results and discussion

3.1. Structural characteristics

As mentioned in the Experimental Section, the $Pd[PPh_2(CH_2)_2Si(OCH_2CH_3)_3]_2Cl_2$ was prepared from $Pd(COD)Cl_2$ and $PPh_2CH_2CH_2Si(OCH_2CH_3)_3$ under argon protection. Then, the organopalladium(II) functionalized SBA-16, denoted as Pd(II)-PMO-SBA-16, was prepared by co-condensation from as obtained $Pd[PPh_2(CH_2)_2Si(OCH_2CH_3)_3]_2Cl_2$ and tetraethyl orthosilicate (TEOS). Pd(II)-PMO-SBA-16 and Pd(II)-PMO-SBA-15 are almost 2 μm in length and 500 nm in diameter. They were determined by SEM analysis.

The elemental analysis gives a composition of C (55.24%) and

H (6.57%) in the $Pd[PPh_2(CH_2)_2Si(OCH_2CH_3)_3]_2Cl_2$ sample, which is in good accordance with that calculated from $C_{60}H_{87}O_9Cl_2P_3PdSi_3$ *C* (55.18%)and H (6.67%). ICP analysis shows P/Pd molar ratio of 2.03. The Pd(II) organometallic complex incorporated into the silica matrix by the co-condensation approach was demonstrated by FTIR, solid-state NMR, and TG-DTA. Fig. 1 shows the FTIR spectra of Pd(II)-PMO-SBA-16. No significant signals indicative of P123 surfactant molecules were observed, implying they were completely removed by EtOH extraction. The Pd(II)-PMO-SBA-16 displayed two peaks at 2985 and 2919 cm^{-1}, which could be attributed to the asymmetric and symmetric stretching modes of C-H bonds. [30] The peak at 693 cm^{-1} was characteristic of the -H out-of-plane deformation of the monosubstituted benzene ring. The peak around 1436 cm^{-1} was assigned to the vibrations of P-CH_2.[31] These results demonstrated the successful incorporation of the Pd(II) organometallic complex into the silica supports. The absorption peak at 1130-1090 cm^{-1} which was indicative of the P-Ph vibration could not be clearly distinguished due to the overlap by the intense Si-O vibration bands at 1100 cm^{-1}.[30] The incorporation of the Pd(II) organometallic complex into the SBA-16 network could be further suggested by solid-state NMR spectra.

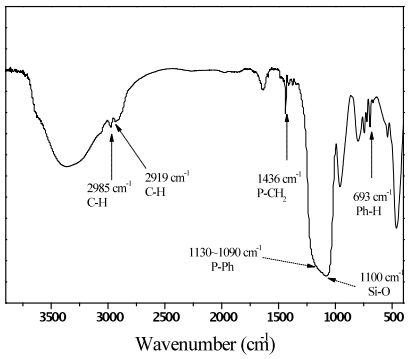

Fig. 1. FTIR spectra of Pd(II)-PMO-SBA-16.

As shown in Fig. 2, the ^{13}C CPMAS NMR spectrum of the Pd(II)-PMO-SBA-16 sample displays two peaks at 14 and 57 ppm were assigned to two C atoms in -CH_2-CH_2-PPh_2 group. A broad peak around 128 ppm was assigned to the C atoms in the benzene ring.[32, 33] Meanwhile, the ^{29}Si MAS NMR spectrum of the Pd(II)-PMO-SBA-16 sample displayed three resonance peaks up-field corresponding to Q^4 (δ = -112 ppm), Q^3 (δ = -102 ppm), Q^2 (δ = -94 ppm) and two peaks down-field corresponding to T^3 (δ = -66 ppm) and T^2 (δ = -59 ppm), where Q^n = $Si(OSi)_n$-$(OH)_{4-n}$, n = 2 ~ 4 and T^m = $RSi(OSi)_m$-$(OH)_{3-m}$, m = 1 ~ 3.[33] The presence of T^m peaks suggested the successful incorporation of the organic silica moieties as a part of the silica wall structure.

This was further suggested by the TG/DTA analysis. As shown in Fig. 3, besides a weight loss due to the removal of physisorbed water, and/or ethanol remained from solvent extraction processes, the Pd(II)-PMO-SBA-16 displayed two peaks around 383 and 452 °C, possibly owing to the successive breakage of two PPh_2-Pd-PPh_2 bonds,[24] corresponding to total weight loss around 16%.

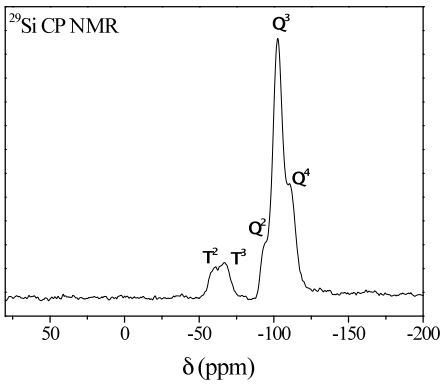

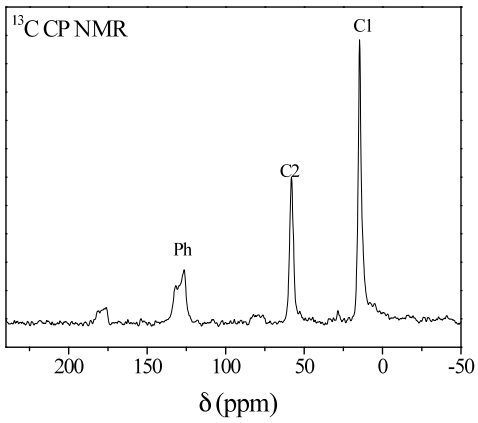

Fig. 2. Solid NMR spectra of Pd(II)-PMO-SBA-16.

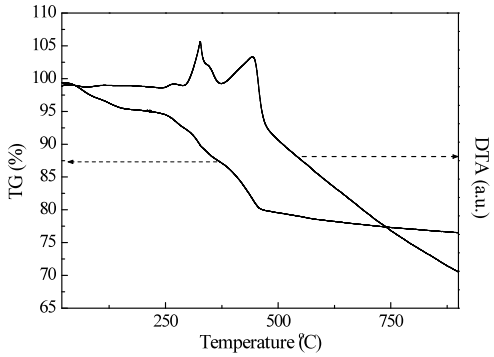

Fig. 3. TG and DTA curves of Pd(II)-PMO-SBA-16.

As shown in Fig. 4, the XPS spectra demonstrated that all the Pd species in the Pd(II)-PMO-SBA-16 were present in +2 oxidation state rather than in metallic state, corresponding to the binding energy (BE) of 343.1 and 337.8 eV in the Pd $3d_{5/2}$ and $3d_{3/2}$ levels,[34] respectively. In comparison with the BE of

the Pd in $Pd(PPh_3)_2Cl_2$, the BE of the Pd in the Pd(II)-PMO-SBA-16 shifted negatively by 0.51 eV, indicating that the $PPh_2CH_2CH_2$- ligand exhibited stronger electron-donation than the PPh_3-ligand, making the Pd atom in the Pd(II)-PMO-SBA-16 more electron-enriched. This can be easily understood by considering the conjugated p-p system between P and Ph-. The PPh_3-ligand displayed a conjugated p-p system comprised of one P atom and three Ph groups while the PPh_2-CH_2-CH_2-ligand exhibits a conjugated p-p system comprised of one P atom and two Ph groups.[29] The bigger conjugated p-p system might dilute electron density on the P atom, which weakens the electron donation ability of the P atom to the Pd atom in the coordination bonds.[32]

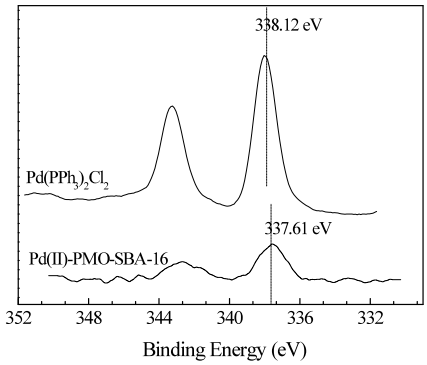

Fig. 4. XPS spectra of $Pd(PPh_3)Cl_2$ and Pd(II)-PMO-SBA-16.

The small-angle XRD pattern of Pd(II)-PMO-SBA-16 in Fig. 5 exhibits a significant peak at 0.7° corresponding to (1 1 0) reflection and comparatively unresolved peaks at 2θ values in the range of 1.0~2.0°, these peaks are related to the Im3m cubic body centered space group, thus providing an indication of the Im3m structure of SBA-16.[35] TEM images (Fig. 6) further confirmed the present of ordered cubic mesostructure group of Pd(II)-PMO-SBA-16.

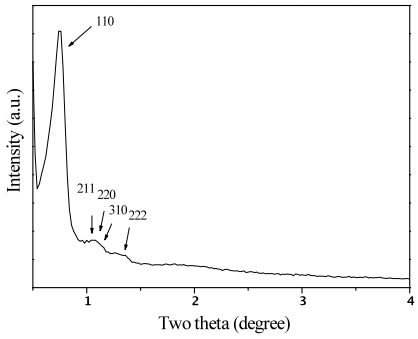

Fig. 5. Low-angle XRD patterns of Pd(II)-PMO-SBA-16.

Fig. 7 illustrates the nitrogen adsorption/desorption isotherms of Pd(II)-PMO-SBA-16 sample. The prepared samples exhibit type-IV N_2 sorption isotherms with H_2-type hysteresis loop characteristic of mesoporous materials with cage-type porous structure suggesting the existence of ink-bottle pores in the above sample.[36] Pore size distribution evaluated from the adsorption branch of the N_2 isotherm by the Barrett-Joyner-Halenda method (Fig. 7 insert) shows the primary mesopores of SBA-16 at the diameter of 6.4 nm, with volume of mesopores and specific surface area estimated to be 0.51 cm^3/g and 676 m^2/g, respectively.

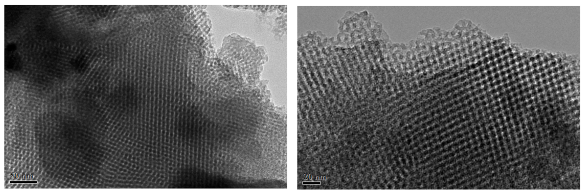

Fig. 6. TEM images of Pd(II)-PMO-SBA-16.

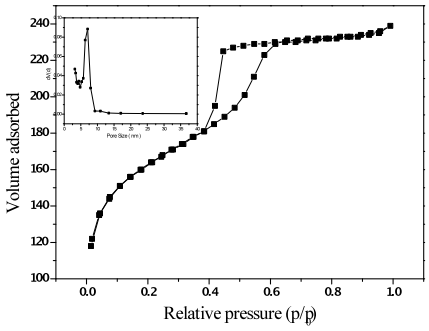

Fig. 7. N_2 adsorption-desorption isotherm of Pd(II)-PMO-SBA-16.

A key consideration of the Pd(II)-PMO-SBA-16 catalyst is the location of Pd(II) species since they should contact with reactant molecules. To determine the chemical accessibility of the Pd(II) organometals incorporated into the silica framework, the oxidation of Pd(II)-PMO-SBA-16 in $KMnO_4$ aqueous solution was attempted. The Pd(II) content determined by $KMnO_4$ oxidation could be considered as accessible Pd(II) species while the total Pd(II) content was determined by ICP analysis. Their molar ratio was determined as 92%, suggesting that most Pd(II) species in the Pd(II)-PMO-SBA-16 catalyst were accessible for chemical in liquid phase reaction.

3.2. Catalytic performances

In order to test the catalytic activity of Pd(II)-PMO-SBA-16 in the Sonogashira coupling reaction, the reaction between iodobenzene and phenylacetylene, was chosen as model reaction using water as solvent to investigate influences of different parameters on the catalytic activity. The parameters included catalyst, catalyst concentration, base, and reaction temperature. The best result was obtained when the cross-coupling was carried out with 6.0 mol % of Pd(II)-PMO-SBA-16 (Table 1, entry 2). The optimized reaction conditions were then applied to the Sonogashira cross coupling reactions of various aryl halides with phenylacetylene (Table 3).

Table 1 The cross-coupling of iodobenzene and phenylacetylene under different conditions.[a]

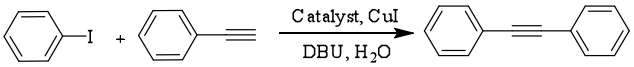

Entry	Catalyst content (mol%)	Base	Temperature (°C)	Yield (%)
1	0.3	DBU	50	62
2	0.6	DBU	70	86
3	0.9	DBU	90	95
4	0.6	Et_3N	90	87
5	0.6	K_2CO_3	90	75
6	0.3	DBU	90	51
7	0.9	DBU	90	97

[a]Reactions conditions: iodobenzene (1.0 mmol), phenylacetylene (1.5 mmol), base, CuI (0.16 mmol), n-decane (2.0 mmol), H_2O (4.0 mL), and Pd(II)-PMO-SBA-16.

Table 2 the catalytic efficiencies of different catalysts in water-medium Sonogashira reaction[a]

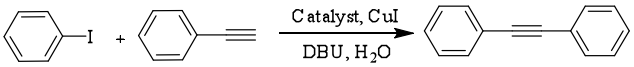

Entry	Catalyst	Yield (%)
1	$Pd(PPh_3)Cl_2$	97
2	Pd(II)-PMO-SBA-16	95
3	Pd(II)-PMO-SBA-15	88

[a]Reactions conditions: iodobenzene (1.0 mmol), phenylacetylene (1.5 mmol), DBU (0.40 mL), CuI (0.16 mmol), n-decane (2.0 mmol), H_2O (4.0 mL), 90 °C and a amount of Pd catalyst.

Table 2 summarized the catalytic parameters of different Pd(II) organometallic catalysts in water-medium Sonogashira reaction. The Pd(II)-PMO-SBA-16 displayed comparable efficiency with the $Pd(PPh_3)_2Cl_2$ homogeneous catalyst. As expected, the reaction catalyzed by the Pd(II)-PMO-SBA-15 catalyst showed slower rate than that of Pd(II)-PMO-SBA-16 catalyst under the same reaction conditions. The reason could be Pd(II)-PMO-SBA-16 containing easy accessible 3D structure consisting of ordered and interconnected spherical mesopores for guest molecules, which facilitates the transport of reactants and products without pore blockage.[25-28]

To make sure whether the heterogeneous or the dissolved homogeneous Pd(II) species were the real catalyst responsible for the coupling reaction between iodobenzene and phenylacetylene, the following procedure was carried out, as proposed by Sheldon et al. [37] According to the proposed method, after reaction for 4 h with the conversion exceeding 45%, the solid catalyst was filtered out and the mother liquor was allowed to react for another 5 h under identical reaction conditions. No significant change in the conversion was observed, indicating that the present catalysis indeed was heterogeneous in nature rather than the dissolved Pd(II) species leached from Pd(II)-PMO-SBA-16.

Table 3 Catalytic efficiencies of the Pd(II)-PMO-SBA-16 in water-medium Sonogashira reactions[a]

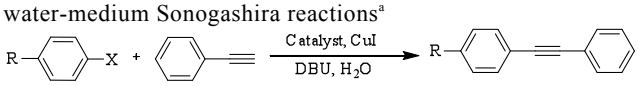

Entry	Catalyst content (mol%)	R	X	Reaction time (h)	Yield (%)
1	0.60	H	I	5	95
2	0.60	CH_3O-	I	7	86
3	0.60	CH_3-	I	7	89
4	0.60	NO_2-	I	4	98
5	0.90	H	Br	8	93
6	0.90	CH_3-	Br	10	85
7	0.90	NO_2-	Br	7	96

[a] Reactions conditions: aryl halide (1.0 mmol), phenylacetylene (1.5 mmol), DBU (0.40 mL), CuI(0.16 mmol), n-decane (2.0 mmol), H_2O (4.0 mL), 90 °C and PMO-SBA-16.

In order to verify the higher activity of Pd(II)-PMO-SBA-16, its activity towards aryl halide containing variation of different substituent with phenylacetylene were examined. These results were summarized in Table 3. The cross-coupling reaction of phenylacetylene with a variety of aryliodides proceeded smoothly, affording high yields at 86-98% (Table 3, entries 1-4). Various electron-donating and electron-withdrawing groups, such as $-OCH_3$ and $-NO_2$ on the aryl iodide were well tolerated. The presence of a strong electron-withdrawing group, such as $-NO_2$, is known to promote the direct coupling. Electron-donating groups, such as $-OCH_3$ on the iodoaryl partner could give excellent results. The results above prompted us to investigate the reaction of aryl bromides. At a catalyst loading of 0.9 mol%, Pd(II)-PMO-SBA-16 also afforded a satisfactory yield for bromides containing $-CH_3$ and $-OCH_3$ groups (Table 3, entries 5-7). Bromoarenes with either electron-withdrawing substituents, such as $-NO_2$ or electron-donating substituents, such as OCH_3 coupled readily with phenylacetylene in good yields. Aryl bromides containing electron-withdrawing substituents reacted faster than those with electron donating substituents (Table 3, entries 6 -7).

3.3. Recycling of the catalyst

One of the purposes for designing this heterogeneous catalyst is to enable recycling of the catalyst for use in subsequent reactions. The reusability of the catalyst was tested upon the reaction phenyliodide with phenylacetylene as the representative reactants and in the presence of 0.60 mol% Pd(II) in order to study the recyclability of this heterogeneous

catalyst. Due to the unavoidable loss of solid catalyst during the course of recovery and washing, we did three parallel reactions at each recycling, then collected all the catalyst and portioned them in the next recycling. Both Pd(II)-PMO-SBA-16 and Pd(II)-PMO-SBA-15 could be repeated for five cycles without significant decrease in the catalytic activity of the catalyst (Fig. 8). The excellent durability of the Pd(II)-PMO-SBA-16 catalyst could be attributed to the Pd(II) organometallic complex embedded in silica walls, which could effectively inhibit the Pd(II)-leaching. According to the ICP analysis, Pd(II) species in the solution was less than 0.5 ppm after being used 5 times, suggesting that the Pd(II)-leaching could be essentially neglected. In addition, On the other hand, the Pd(II) organometals embedded in silica walls might also enhance the hydrothermal stability of Pd(II)-PMO-SBA-16.[38]

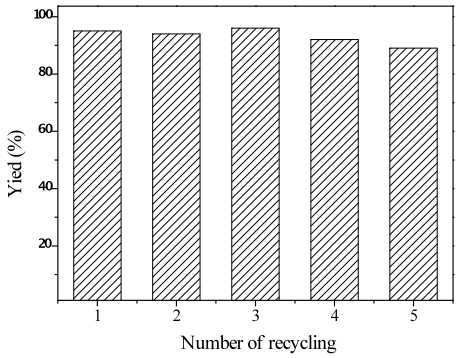

Fig. 8. Recycling tests of Pd(II)-PMO-SBA-16.

4. Conclusions

In summary, we have presented a Pd(II) organometal functionalized SBA-16, which was efficiently used as a heterogeneous catalyst for Sonogashira coupling reactions in water medium. The catalyst not only shows high catalytic activity, but also offers many practical advantages such as thermal stability and recyclability. The catalyst was reused for four runs in Sonogashira reaction without significant loss of activity, indicating good potential for industrial applications. In comparison with those bonded to traditional mesoporous silica supports (e.g., SBA-15), the three-dimensional mesoporous cage-like material SBA-16 was demonstrated to have a superior ability in reducing the diffusion resistance. It can be envisioned that other organometallic catalysts including Rh (I), Ru (II), Ni (II), and rare earth metals can also be designed in this way, which may offer more opportunities for developing powerful and reusable catalysts for green organic synthesis.

Acknowledgements

We are grateful to the National Natural Science Foundation of China (20825724), University Natural Science Foundation of Jiangsu Province (13KJB150008) and Administration of Science & Technology of Huaian city (HAG2013077).

References

1 K. Sonogashira, Metal-Catalyzed Cross-Coupling Reactions; Wiley-VCH: New York, U.S.A., 1998.
2 I. Paterson, R. D. M. Davies and R. Marquez, *Angew. Chem. Int. Ed.,* 2001, **40**, 603.
3 T. Hundertmark, A. F. Littke, S. L. Fu and G. C. Buchwald, *Org. Lett.,* 2000, **2**, 1729.
4 N. D. P. Cosford, L. Tehrani, J. Roppe, E. Schweiger, N. D. Smith, J. Anderson, L. Bristow, J. Brodkin, X. Jiang, I. McDonald, S. Rao, M. Washburn and M. A. Varney, *J. Med. Chem.,* 2003, **46**, 204.
5 K. Sonogashira, Y. Tohda and N. Hagihara, *Tetrahedron Lett.,* 1975, **16**, 4467.
6 R. Chinchilla and C. Na´jera, *Chem. Soc. Rev.,* 2011, **40**, 5084.
7 R. Chinchilla and C. Na´jera, Chem. Rev., 2007, **107**, 874.
8 A. N. Marziale, J. Schlüter and J. Eppinger, T*etrahedron Lett.* 2011, **52**, 6355.
9 A. Komáromi, G.L. Tolnai and Z. Novák, *Tetrahedron Lett.,* 2008, **49**, 7294.
10 X. Z. Wang, J. Zhang, Y. Y. Wang and Y. Liu, *Catal. Commun.,* 2013, **40**, 23.
11 M.O. Simon and C.J. Li, *Chem. Soc. Rev.,* 2012, **41**, 1415.
12 B. Basavaprabhu, M. Samarasimhareddy, G. Prabhu and V. Sureshbabu, *Tetrahedron Lett.,* 2014, **55**, 2256.
13 M. Bakherad, A. Keivanloo, B. Bahramian and S. Jajarmi, *J. Organomet. Chem.*, 2013, **724**, 206.
14 Y. He and C. Cai, *J. Organomet. Chem.*, 2011, **696**, 2689.
15 C. M. Kang, J. L. Huang, W. H. He, F. Zhang, *J. Organomet. Chem.* 2010, **695**, 120.
16 M.J. Jin and D.H. Lee, *Angew. Chem. Int. Ed.,* 2010, **49**, 1119.
17 A.K. Nezhad and F. Panahi, *Green Chem.,* 2011, **13**, 2408.
18 Y. He and C. Cai, *J. Organomet. Chem.,* 2011, **696**, 2689.
19 W.H. He, F. Zhang and H.X. Li, *Chem. Sci.*, 2011, **2**, 961.
20 V. Polshettiwar, C. Len and A. Fihri, *Chem. Rev.*, 2009, **253**, 2599.
21 J. Huang and F. Zhang, Appl. Organometal. Chem., 2010, **24**, 767.
22 E.B. Cho, D. Kim, J. Gorka and M. Jaroniec, *J. Mater. Chem.,* 2009, **19**, 2076.
23 A. Molnár, *Chem. Rev.,* 2011, **111**, 2251.
24 D.Y. Zhao, Q.Huo, J. Feng, B.F. Chmelka and G.D. Stucky, *J. Am. Chem. Soc.,* 1998, **120**, 6024.
25 E. Rivera-Muñoz and R. Huirache-Acuña, *Inter. J. Mol. Sci.,* 2010, **11**, 3069.
26 Y. Sakamoto, M. Keneda, O. Teresaki, D.Y. Zhao, J. Kim and G. Stucky, *Nature,* 2000, **408**, 4493.
27 D.Y. Zhao, J. Feng, Q. Huo, N. Melosh, G. Fredrickson and B. Chmelka, *Science,* 1998, **279**, 548.
28 R. Grudzien, B. Grabicka and M. Jaroniec, *J. Mater. Chem.,* 2006, **16**, 819.
29 X.S. Yang, F.X. Zhu, J.L. Huang, F. Zhang and H.X. Li, *Chem. Mater.,* 2009, **21**, 4925.
30 A. S. M. Chong and X. S. Zhao, *J. Phys. Chem., B* 2003, **107**, 12650.
31 Q. Hu, J. Hampsey, N. Jiang, C. Li and Y. Lu, *Chem. Mater.,* 2005, **17**, 1561.
32 F. Zhang, G.H. Liu, H.X. Li and Y.F. Lu, *Adv. Funct. Mater.,* 2008, **18**, 1.
33 M. Jurgen, G. Martin, W. Georg, J. Jian, H. Michael, J. Peter and F. Michael, *J. Mater. Chem.,* **2006**, **16**, 2809.
34 J. F. Moulder, W. F. Stickle, P. E. Sobol and K. D. Bomben, Handbook of X-ray Photoelectron Spectroscopy, A Reference Book of Standard Spectra for Identification and Interpretation of XPS Data; Perkin-Elmer Corporation, Physical Electronics Division: Eden Prairie, MN, 1992.
35 H. Q. Yang, L. Zhang, W. Su, Q. Yang and C. Li, *J. Catal.,* 2007, **248**, 204.

36 K. Morishige, N. Tateishi and S. Fukuma, *J. Phys. Chem. B,* 2003, **107**, 5177-5181.
37 R. A. Sheldon, *Green Chem.,* 2005, **7**, 267.
38 J. E. Herrera, J. Kwak, J. Z. Hu, Y. Wang, C. H. F. Peden, J. Macht and E. Iglesia, *J. Catal.,* 2006, **239**, 200.